Cardiovascular Flow Measurement with Phase-Contrast MR Imaging: Basic Facts and Implementation[1]

Joachim Lotz, MD • Christian Meier, PhD • Andreas Leppert, MD
Michael Galanski, MD

Phase-contrast magnetic resonance (MR) imaging is a well-known but undervalued method of obtaining quantitative information on blood flow. Applications of this technique in cardiovascular MR imaging are expanding. According to the sequences available, phase-contrast measurement can be performed in a breath hold or during normal respiration. Prospective as well as retrospective gating techniques can be used. Common errors in phase-contrast imaging include mismatched encoding velocity, deviation of the imaging plane, inadequate temporal resolution, inadequate spatial resolution, accelerated flow and spatial misregistration, and phase offset errors. Flow measurements are most precise if the imaging plane is perpendicular to the vessel of interest and flow encoding is set to through-plane flow. The sequence should be repeated at least once, with a high encoding velocity used initially. If peak velocity has to be estimated, flow measurement is repeated with an adapted encoding velocity. The overall error of a phase-contrast flow measurement comprises errors during prescription as well as errors that occur during image analysis of the flow data. With phase-contrast imaging, the overall error in flow measurement can be reduced to less than 10%, an acceptable level of error for routine clinical use.

Abbreviations: IVC = inferior vena cava, ROI = region of interest, SVC = superior vena cava

Index terms: Blood, flow dynamics, 56.12144, 94.12944 • Magnetic resonance (MR), phase imaging, 56.12144, 94.12944 • Magnetic resonance (MR), vascular studies, 56.12144, 94.12944

RadioGraphics 2002; 22:651–671

[1]From the Department of Diagnostic Radiology, Medical School Hannover, Carl-Neuberg-Strasse 1, D-30625 Hannover, Germany. Presented as a scientific exhibit at the 1999 RSNA scientific assembly. Received October 1, 2001; revision requested December 6 and received January 21, 2002; accepted January 21. **Address correspondence to** J.L. (e-mail: *lotz.joachim@mh-hannover.de*).

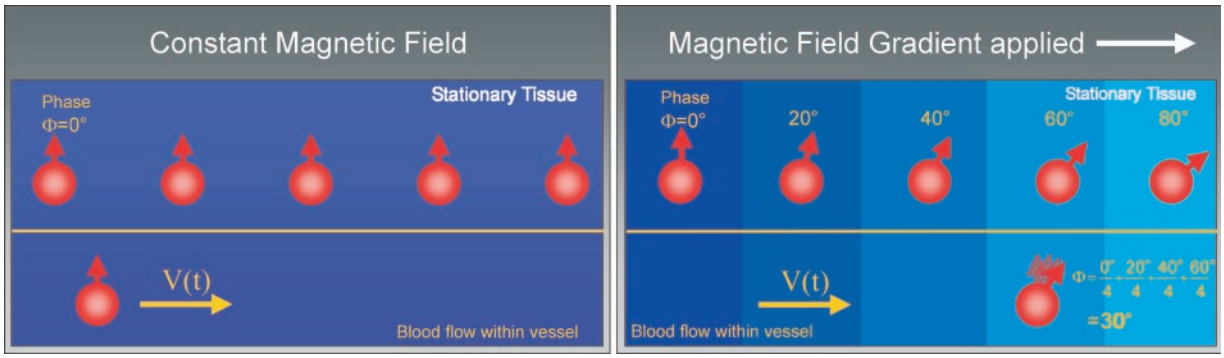

Figure 1. Diagrams show that spins moving along an external magnetic field gradient acquire a difference in the phase of their rotation (right), whereas nonmoving spins do not (left). The amount of phase difference is proportional to the velocity of the moving spin. t = time, V = velocity, Φ = phase shift.

Introduction

Quantitative flow measurement has been used by magnetic resonance (MR) imagers since the 1980s (1–3), and its potential has been known since about 1960 (4). The need for postprocessing and the high availability of Doppler flow units have limited the use of phase-contrast MR imaging in cardiovascular imaging. However, with the increasing power of MR imaging units and the reduced time needed to complete a cardiac study, more and more indications are evolving for use of phase-contrast flow measurements as an additional source of quantitative functional information in cardiac MR imaging (5–8).

In this article, we discuss the basics of phase-contrast imaging and prospective and retrospective gating techniques, describe the errors and limitations associated with phase-contrast imaging, provide guidelines for measurement and data analysis, and present specific protocols.

Basics of Phase-Contrast Imaging

Magnetic moments (which are hereafter referred to as *spins*) moving along a magnetic field gradient acquire a shift in their phase of rotation in comparison to stationary spins (Figs 1, 2). For linear field gradients, the amount of this phase shift Φ is proportional to the velocity of the moving spin (9). Phase shifts of stationary tissue are compensated for with the help of a bipolar gradient. By repeating the measurement with an inverted bipolar gradient, phase shifts induced by other sequence parameters are eliminated (10). The phase difference that remains after subtraction of these two data sets is used for a voxelwise calculation of velocities (11).

Phase shifts are measured in degrees, and their values should be within a range of ±180°. Therefore, the user has to tune the sequence to the peak velocity expected in the vessel of interest before starting the measurement. By entering this threshold value as the encoding velocity, the amplitudes of the flow-sensitizing gradients are calculated so that the peak velocity corresponds to a phase shift of 180°. The velocity v can be determined by the phase difference $\Delta\Phi$ acquired in the two interleaved measurements:

$$\Delta\Phi = \gamma \cdot \Delta m \cdot v, \qquad (1)$$

where γ is the gyromagnetic ratio and Δm denotes the difference of the first moment of the gradient-time curve. For rectangular bipolar gradient pulses, m simply means the product of the gradient area and the time between the two lobes of the bipolar gradient.

Velocity encoding (V_{enc}) is given in centimeters per second. It determines the highest and lowest detectable velocity encoded by a phase-contrast sequence. Therefore, V_{enc} = 100 cm/sec describes a phase-contrast experiment with a measurable range of flow velocities of ±100 cm/sec.

V_{enc} is inversely related to the area of the flow-encoding gradients. Hence, for the imaging time to remain unchanged, stronger gradient amplitudes are required to encode smaller velocities.

In terms of the physics, it is the transverse component of the spin magnetization that can acquire a motion-induced phase shift. Therefore, it is necessary to first induce a transverse magnetization with the help of a radio-frequency pulse before the flow-sensitizing gradients can be applied.

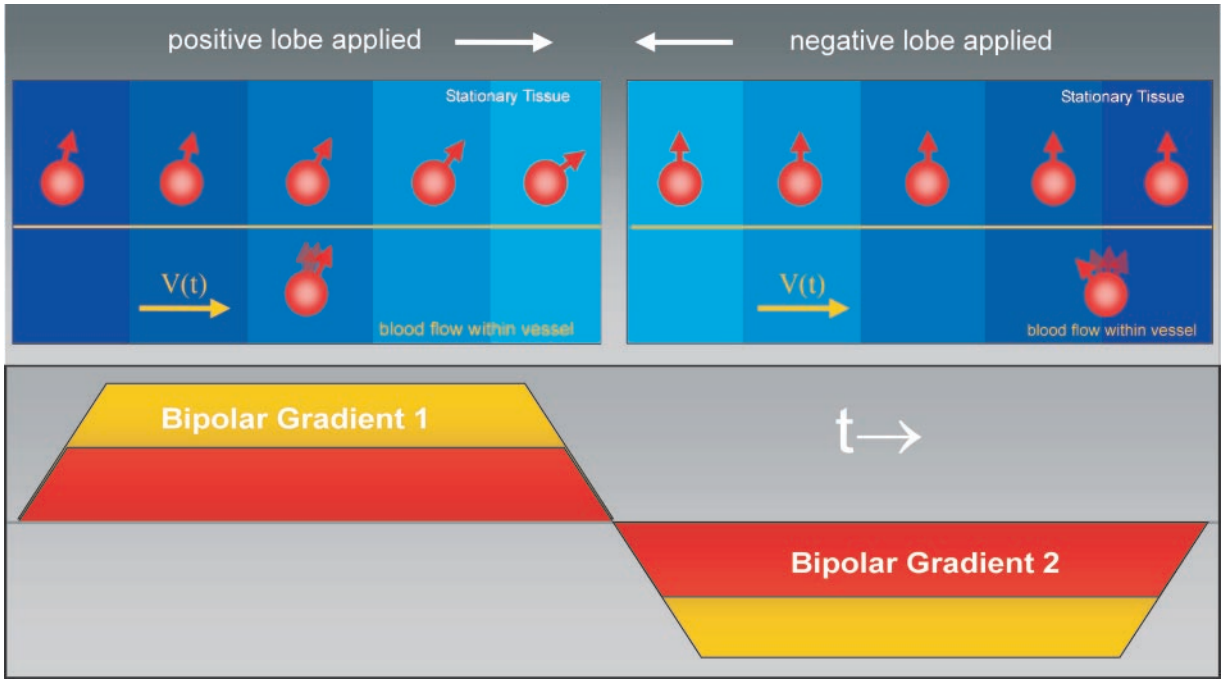

Figure 2. Principle of phase-contrast sequences available in most clinical MR imaging units. Diagram shows that two acquisitions are performed, each one with all parameters kept constant except for the flow-sensitizing bipolar gradients. The data of the two acquisitions are subtracted. The effective flow encoding is achieved by means of the difference in the bipolar gradients of the two acquisitions. This technique eliminates all phase shifts induced by imaging gradients. t = time, V = velocity.

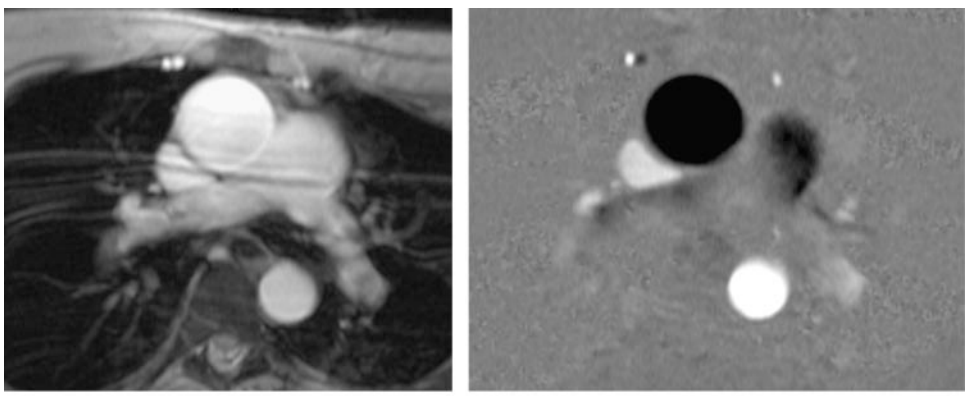

a. **b.**

Figure 3. The information from phase-contrast measurement is processed into two sets of images. **(a)** A magnitude image resembles a normal bright-blood image. It is used for anatomic orientation. **(b)** In a velocity image, the gray value of each pixel represents the velocity information in that voxel. Black values show flow toward the viewer, whereas white values show flow away from the viewer; the image is not standardized to flow toward or away from the heart. The thoracic skeletal muscles can be used to get an impression of the noise in the image. Phase information for air (as in lung tissue) is arbitrary and cannot be used for background subtraction or estimation of noise.

Every MR imaging data acquisition yields information about the signal magnitude as well as the phase of each voxel. Signal intensities are processed into an anatomic image: the *magnitude image*. In conventional imaging sequences, the phase information is discarded because the phase in the individual voxel is arbitrary. In phase-contrast measurement, the phase information is used to calculate the velocity in each voxel in the form of a phase or *velocity image* (Fig 3).

Prospective and Retrospective Gating Techniques

There are two different techniques for synchronizing the measurement of MR imaging data with the cardiac cycle. Both techniques require a trigger signal (eg, the R peak of an electrocardiographic waveform or the systolic peak of a pulsimeter).

Prospective gating techniques wait for a trigger signal to start the data acquisition. At the end of each cardiac cycle, data collection is paused and the sequence waits for the next trigger signal to come. This time interval is called the *arrhythmia rejection window*. It is used to compensate for physiologic variations in the length of the cardiac cycles during measurement. By truncating the cardiac cycle to a constant length, the sequence can be made insensitive to mild arrhythmia. As a trade-off, the flow of late diastole may not be measured correctly, since data are not sampled during the arrhythmia rejection window. This might be of importance in evaluation of the coronary arteries or pathologic conditions of the atrioventricular valves, where flow is maximal during diastole. Most phase-contrast sequences that can be performed in a breath hold use prospective gating techniques.

In retrospective gating techniques, data collection is done continuously throughout the whole cardiac cycle. During image reconstruction, the recorded trigger signals are used to retrospectively assign the data to the different positions in the cardiac cycle. As with prospective gating techniques, the data on flow measurement are collected during more than one cardiac cycle. Since there are always physiologic variations in the length of the cardiac cycles, the data have to be interpolated to represent a mean cardiac cycle. As a trade-off, small inaccuracies due to data interpolation are inherent to retrospective gating techniques. The major advantage of retrospective gating techniques is the ability to provide data from the whole cardiac cycle. Most phase-contrast sequences that can be performed during normal breathing use retrospective gating techniques.

Whether a sequence uses prospective or retrospective gating techniques usually cannot be determined from the phase-contrast images. This information is usually given in the sequence manuals of the MR imaging system.

Errors and Limitations

A drawback of all techniques for measuring blood flow velocity in vivo is the lack of a standard of reference. Flow measurements made in vivo are only approximations based on results of phantom studies (12). Therefore, the overall error of phase-contrast measurements is difficult to estimate. Using phase-contrast measurement, Evans et al (13) found a 5% difference between flow in the ascending aorta and flow in the pulmonary artery in healthy volunteers. A deviation from the true flow of 3.5%–4.5% was estimated as the inborn technical error of phase-contrast measurement when a non–breath-hold cine gradient-echo sequence with prospective gating is used. Kondo et al (14) found similar deviations between flow in the aorta and flow in the pulmonary trunk. Using retrospective gating and a breath-hold sequence (FastCine PC; GE Medical Systems, Milwaukee, Wis), we found a 3% difference between flow in the ascending aorta and flow in the pulmonary artery with an intraobserver variability of 2% and interobserver variability of 3% (data not published).

In comparison, results of the phase-contrast method correspond well to results of Doppler ultrasonography (US) and show fair correspondence to results of invasive techniques based on thermodilution, the ink-indicator method, or the Fick principle (14,15).

Besides being invasive, these techniques are highly operator dependent and sensitive to respiratory volume changes (16). For thermodilution techniques, tricuspid valve insufficiency can cause large deviations from true flow of as much as 80% (17). Studies that directly compared flow measurement with invasive techniques versus MR imaging techniques showed significant discrepancies between the different techniques (18,19). Only recently, we have found a better correspondence between phase-contrast measurement and a modified thermodilution technique, with an overall difference of approximately 10% for measurement of cardiac output (15).

More relevant in daily practice is the comparison with Doppler US. In recent studies, phase-contrast flow measurement showed lower peak velocities in comparison with Doppler US (20). However, it has been reported that Doppler US tends to overestimate peak velocities by as much as 25% (21).

Phase-contrast techniques have been shown to be superior to Doppler US with respect to measurement of mean flow. Doppler US assumes a constant velocity over the whole vessel area. However, MR imaging can take into account the variation of flow in the vessel within the specified spatial resolution. This is why Doppler US tends to overestimate the mean flow in larger vessels (13,22,23).

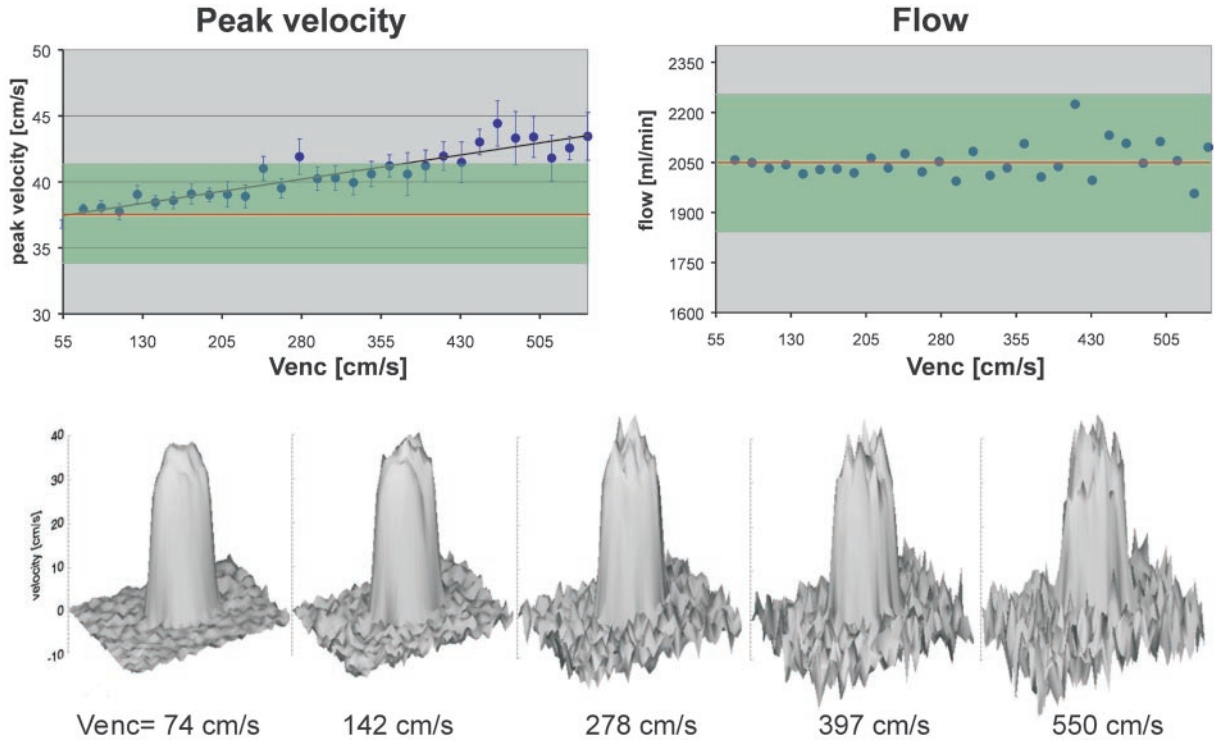

Figure 4. Effect of a mismatched V_{enc} on noise. Top: Graphs show that, in an experimental setting, estimates of peak velocity demonstrate a deviation of more than 10% if V_{enc} increases by more than three times the velocity in the vessel (left), whereas estimates of flow are largely preserved (right). Red line indicates the true peak velocity or true flow. Green area indicates a deviation of 10% from the true peak velocity or true flow. Bottom: Surface renderings of data from velocity images obtained at different values of V_{enc} show how increasing noise may mask the true peak velocity values. (The experimental setting consisted of the following: laminar steady flow of 2.05 L/min, gadolinium-doped saline solution, and a 1.5-cm-diameter glass tube. The real flow rate was monitored with an inductive flowmeter. The imaging parameters were kept constant while V_{enc} was varied between 57 cm/sec and 550 cm/sec.)

With the sequences available for routine clinical use, phase-contrast measurement is not able to provide real-time velocity information. Instead, all measured velocities are averaged over a range of cardiac cycles. This may be a benefit when evaluating the flow averaged over a longer time (eg, to compensate for respiratory changes in venous blood flow). Information on peak velocities under various physiologic conditions (eg, the Valsalva maneuver) can be obtained with MR imaging (22) but is more easily acquired with real-time Doppler US.

The clinical relevance of these principal differences must be discussed with caution, as each technique per se gives reasonable and clinically useful results. However, whenever diverging results from different modalities for flow measurement are discussed, knowledge of the technical limitations can help one find the most sensible result in the given situation.

In the remainder of this section, the most common and avoidable mistakes in phase-contrast measurement are discussed. Knowledge of these mistakes should help keep the overall error in flow measurement to below 10%, which is an acceptable level of error for routine clinical use.

Mismatch of Encoding Velocity

Encoding Velocity Too High (Noise).—The better the encoding velocity matches the real velocity of the region of interest, the more precise the measurement becomes.

Quantification of flow always requires consideration of the noise (ie, the random error of phases). The noise in a velocity image σ is determined by the flow-encoding velocity and the signal-to-noise ratio (SNR) of the magnitude images (24):

$$\sigma \sim \frac{V_{enc}}{SNR}. \quad (2)$$

Noise in velocity images increases with larger V_{enc} values (Fig 4). Peak velocity estimates are

Figure 5. Difference in diastolic flow estimates in a healthy volunteer. The cardiac output was 6.5 L/min as determined with phase-contrast measurement in the ascending aorta. V_{enc} was optimized for systolic flow (V_{enc} = 120 cm/sec). Left: Graph shows the flow curve. Green area indicates the diastolic interval. Measurement was repeated with V_{enc} optimized for diastolic flow (V_{enc} = 40 cm/sec). Right: Graph shows the diastolic flow values obtained with each V_{enc} value. The difference between the measurements was about 4%.

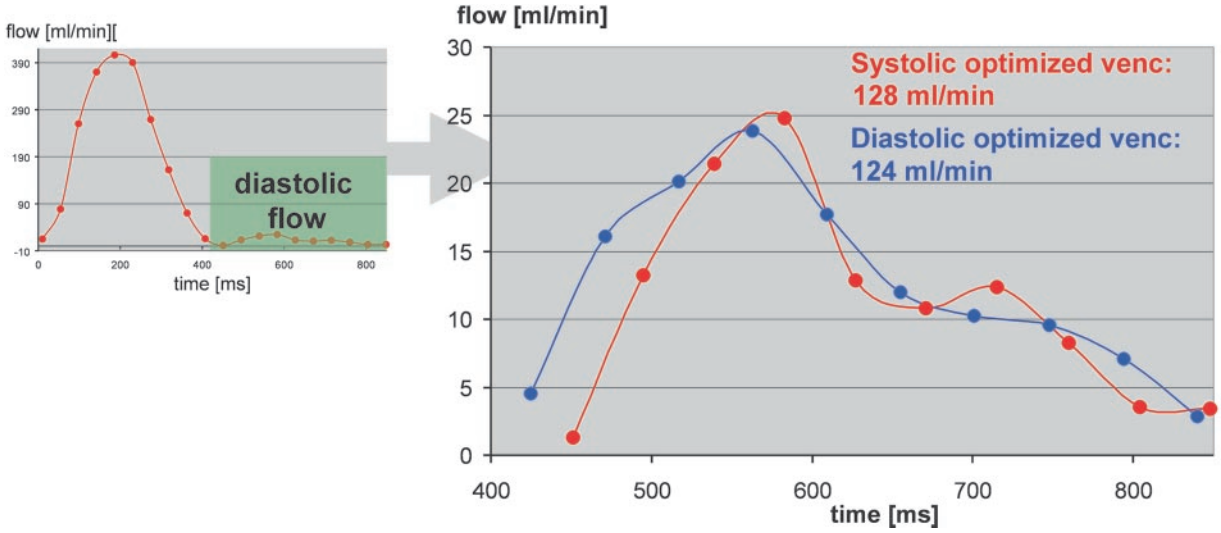

more affected than estimates of flow. Noise affects estimation of the peak velocity V_{max} because it may be masked by noise peaks. Noise has less influence on estimation of flow because the noise is averaged over a number of voxels. Therefore, larger deviations from the ideal V_{enc} can be tolerated as long as the peak velocity is not the main interest of the measurement.

It has been reported that slow flow in the aorta, as is encountered during diastole, may be systematically underestimated if the V_{enc} chosen is too large (13,23). However, when sequences with an optimized signal-to-noise ratio are used, the resulting error is less than 10% (Fig 5). This error is acceptable in daily practice; thus, more sophisticated improvements, such as dynamic velocity encoding during the cardiac cycle (23), have not yet attracted attention for routine clinical use.

As can be seen in Equation (2), noise in a velocity image also depends on the signal-to-noise ratio of the magnitude image. An increased signal-to-noise ratio for magnitude images can be achieved by optimizing sequence parameters like section thickness, flip angle, and echo time and the receiver bandwidth. However, increasing the echo time makes the sequence more vulnerable to motion artifacts, and an increase in the section thickness may induce significant partial volume effects in smaller vessels like the coronary arteries or bypass vessels.

Encoding Velocity Too Low (Aliasing).—Setting the encoding velocity below the peak velocity in the vessel of interest results in aliasing. Basically, aliasing is a wrapping around of velocity information within a voxel (Fig 6).

Aliasing may have deleterious effects on the results of flow measurement. Fortunately, it is the easiest error to detect in flow measurements. It can be perceived in the velocity images, in which the voxels of assumed peak velocities have an inverted signal intensity compared with that of surrounding voxels (Figs 6, 7).

Aliasing can be corrected with some software packages if the peak velocity stays in a reasonable range of smaller than three times the V_{enc} (25). If such software is not available, manual correction can be performed, especially when one is evaluating peak velocities only (Fig 8). However, it is safer and often more efficient to repeat the flow measurement with a modified V_{enc} than to correct the aliased data set.

Figures 6, 7. **(6)** Aliasing in flow measurements from the ascending aorta. Top: Magnitude images. Middle: Corresponding velocity images. Aliasing (arrow) is seen in the image obtained with a V_{enc} of 100 cm/sec (left) but not in the image obtained with a V_{enc} of 120 cm/sec (right). Bottom: Corresponding profile plots along the red lines in the velocity images show that velocities beyond $V_{enc} = -100$ cm/sec wrap around from the other side of the velocity range defined by the V_{enc}. **(7)** Periodicity of aliasing in an experiment with laminar flow of 1.7 L/min and peak velocity (V_{max}) of 320 cm/sec. In repeated measurements, V_{enc} was decreased from $V_{enc} = V_{max}$ to $V_{enc} = 1/8\ V_{max}$. **(a)** Magnitude images (right) and velocity images (middle) obtained with different V_{enc} values and corresponding profile plots along the red lines in the velocity images (left). **(b)** Graph shows the mean flow determined at various values of V_{enc}. The absolute flow values decrease rapidly with increasing aliasing. **(c)** Graph shows the peak velocity of aliased voxels determined at various values of V_{enc}. Below $V_{enc} = 1/3\ V_{max}$, the velocity of aliased voxels seems to follow the V_{enc} values. Aliasing at values of V_{enc} below $1/3\ V_{max}$ cannot be corrected by hand or with software packages.

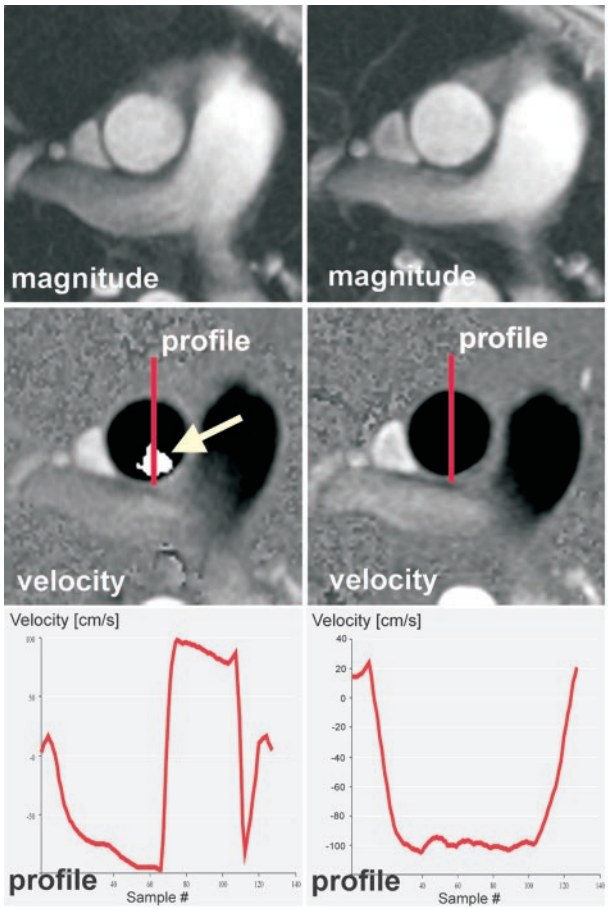

6.

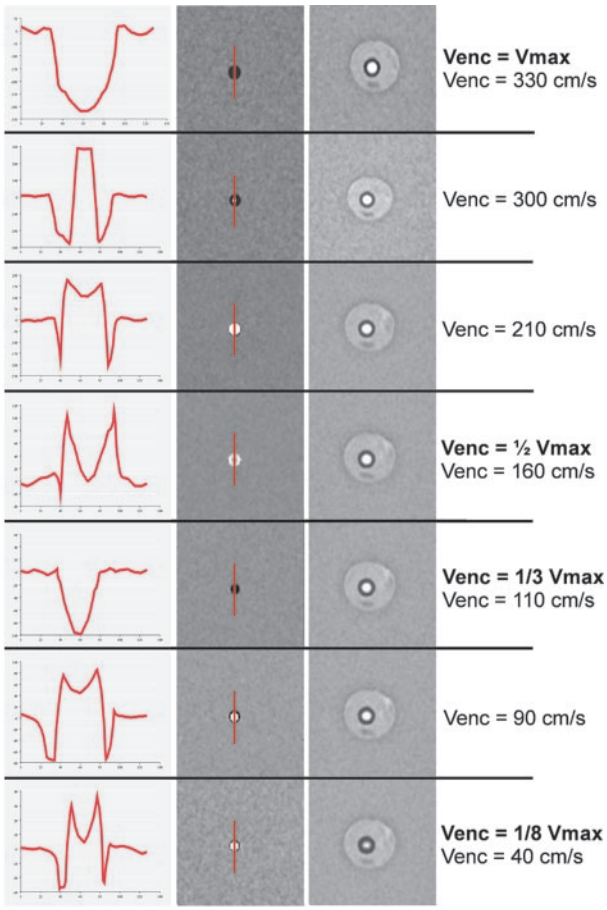

7a.

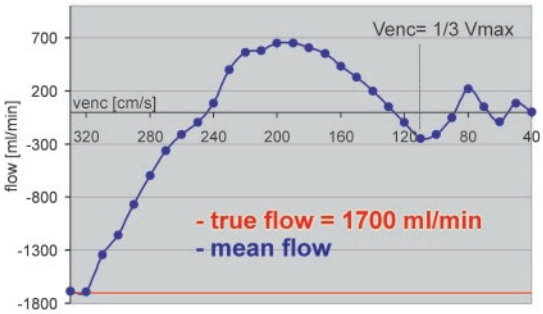

7b.

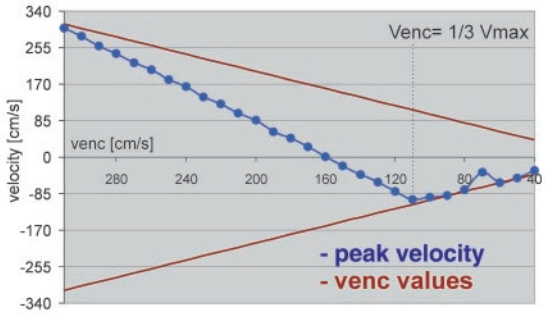

7c.

Figure 8. Manual correction of aliasing in evaluation of peak velocity. **(a)** Magnitude (top left) and velocity (top right) images of the ascending aorta. There is aliasing in the velocity image, which was obtained with a V_{enc} of 100 cm/sec. Bottom left: Magnified view of the velocity image above. A region of interest (ROI) is defined that includes only the aliased voxels (red shaded area). In this ROI, the lowest velocity value V_{min} is determined (arrow). Far right: Profile plot along the red line in the velocity image. The dotted line indicates the expected velocity values that have aliased. **(b)** The true peak velocity is calculated as the sum of V_{enc} and Δv (Δv is the difference between V_{enc} and V_{min}). This is a simple, practical approach that allows the user to account for the positive or negative value of the final value of V_{max}.

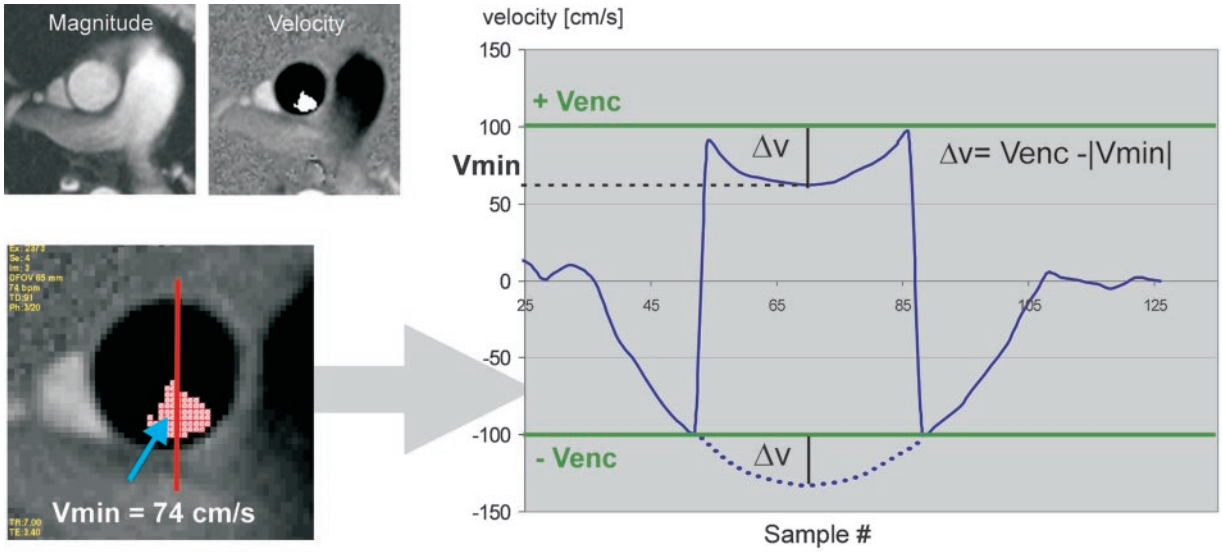

a.

Vmax = Venc + Δv

simplified for daily use:

Vmax = 2 x Venc – |Vmin|

in this example

Vmax = 2 x 100 – 74 = 126 cm/s

b.

Deviation of Imaging Plane

Measurements of flow are most precise if the imaging plane is positioned orthogonal to the main direction of flow and through-plane flow encoding is used. In-plane flow encoding should not be used for estimation of flow because of increased partial volume effects and the inability to visualize the whole diameter of the vessel.

Measurement of peak velocity can be performed with any flow-encoding direction (in-plane or through-plane flow encoding) as long as the direction of flow encoding matches the direction of maximum blood flow.

Deviation of ±15° from the orthogonal imaging plane is tolerable for estimation of flow. Up to this angle, the increase in vessel area is compensated for by the increase in partial volume effects (26) (Fig 9).

An ovoid shape of an arterial vessel usually signifies gross deviation from the ideal orthogonal imaging plane. However, ovoid contours can be found in the venous system and sometimes in shunt vessels or other vascular prostheses.

Deviations from the imaging plane might remain unnoticed in double oblique prescriptions for stenotic jets if there are no reference structures for orientation.

Inadequate Temporal Resolution

Cardiac-gated flow measurement yields a set of images or *frames*, each of which shows the anatomy and velocity information at a different point of time in the cardiac cycle. The sequences used in most clinical imaging units employ the tech-

Figure 9. Deviation from the ideal imaging plane. Top: Graphs show how estimates of peak velocity (left) and flow (right) are affected by deviation of the imaging plane from the ideal orthogonal orientation relative to the flow direction. Deviations of more than 15° cause significant deviations from both the peak velocity and flow rate of more than 10% (green area). (The experimental setting consisted of the following: constant laminar flow, tube diameter of 1.5 cm, 1-mm wall thickness, and flow rate of 1.7 L/min. The fluid was gadolinium-doped saline solution. A commercially available sequence [FastCine PC; GE Medical Systems] was used, and retrospective electrocardiographic gating was performed at a heart rate of 90 beats per minute with an artifical gating device.) Bottom: Magnitude images (right) obtained at various deviations from the orthogonal imaging plane (left). Deviations of less than 15° may not be detected on the magnitude images.

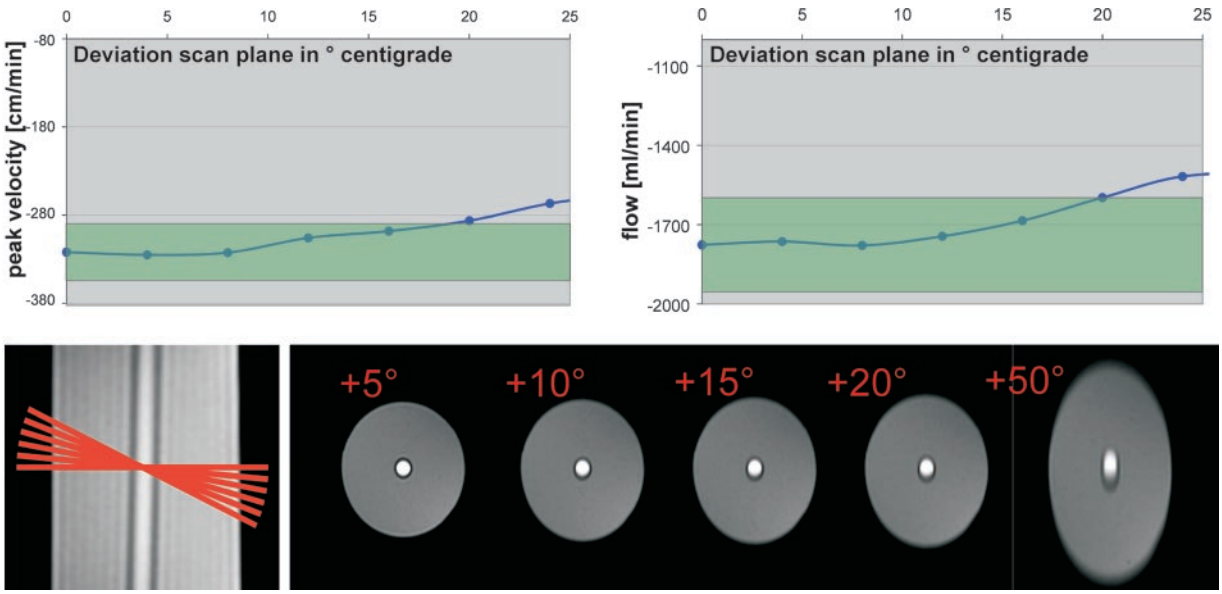

nique of k-space segmentation to acquire the data of all frames as fast as possible: Within each heartbeat, a certain number of k-space lines are sampled for each frame. This number is called the views per segment (VPS). The time resolution T_{res} of such a phase-contrast sequence is defined as follows:

$$T_{res} = 2 \cdot TR \cdot VPS, \quad (3)$$

where TR is the repetition time. The factor 2 is the result of the sequence design (27). As mentioned earlier (in the section entitled "Basics of Phase-Contrast Imaging"), each k-space line is sampled twice by using the same repetition time (11) and the data of the two acquisitions are subtracted. This is true for almost all available phase-contrast sequences.

In some systems, even more frames than initially obtained are produced by linear interpolation of the data of two adjacent frames. This technique is known as *view sharing* (28). View sharing can improve the temporal resolution of the measurement up to an effective resolution of $T_{eff} = 2 \cdot TR$ (27), although the true temporal resolution of the data collected is not changed. View sharing can be defined as a technique for using the collected data more efficiently.

Whereas the views per segment value can be set by the user, the degree of view sharing is accessible to the user only if the sequence has the option of modifying the number of cardiac frames to be reconstructed from the acquired data. The higher the number of cardiac frames, the more interpolation (ie, view sharing) is used.

In most sequences available, the number of frames to be reconstructed is calculated by the imaging unit and cannot be altered by the user. This is true for most of the sequences designed for measurement in a breath hold. However, if the number of frames to be reconstructed can be controlled by the user, the optimal value is largely dependent on the views per segment value used in the sequence. For most situations, a value of 30 frames is sufficient, representing a good compromise between waste of disk space, time for postprocessing, and the temporal accuracy of the flow measurement.

When a low temporal resolution is used, the peak velocity and flow in the great arteries are underestimated (Fig 10).

Figure 10. Temporal resolution (number of reconstructed images). A healthy volunteer was imaged by using a V_{enc} of 120 cm/sec, a commercially available sequence (FastCine; GE Medical Systems), retrospective gating, and k-space segmentation with eight views per segment. A cardiac output of 4.9 L/min was determined with phase-contrast measurement in the ascending aorta. The experiment was repeated with a decreasing number of reconstructed cardiac frames. **(a)** Graph shows the flow curves for six and 40 reconstructed frames per cardiac cycle. **(b, c)** Graphs show the changes in measured peak velocity **(b)** and cardiac output **(c)** at various numbers of reconstructed frames per cardiac cycle. Reconstruction of more than 16 frames per cardiac cycle did not improve the accuracy of the data set. Green area indicates a deviation of ±10% from the peak velocity or cardiac output at the highest temporal resolution. The lower the views per segment value, the greater the number of frames to be reconstructed to achieve optimal accuracy. Selection of 30 frames per cycle as a standard value covers all ranges from two views per segment to 14 views per segment.

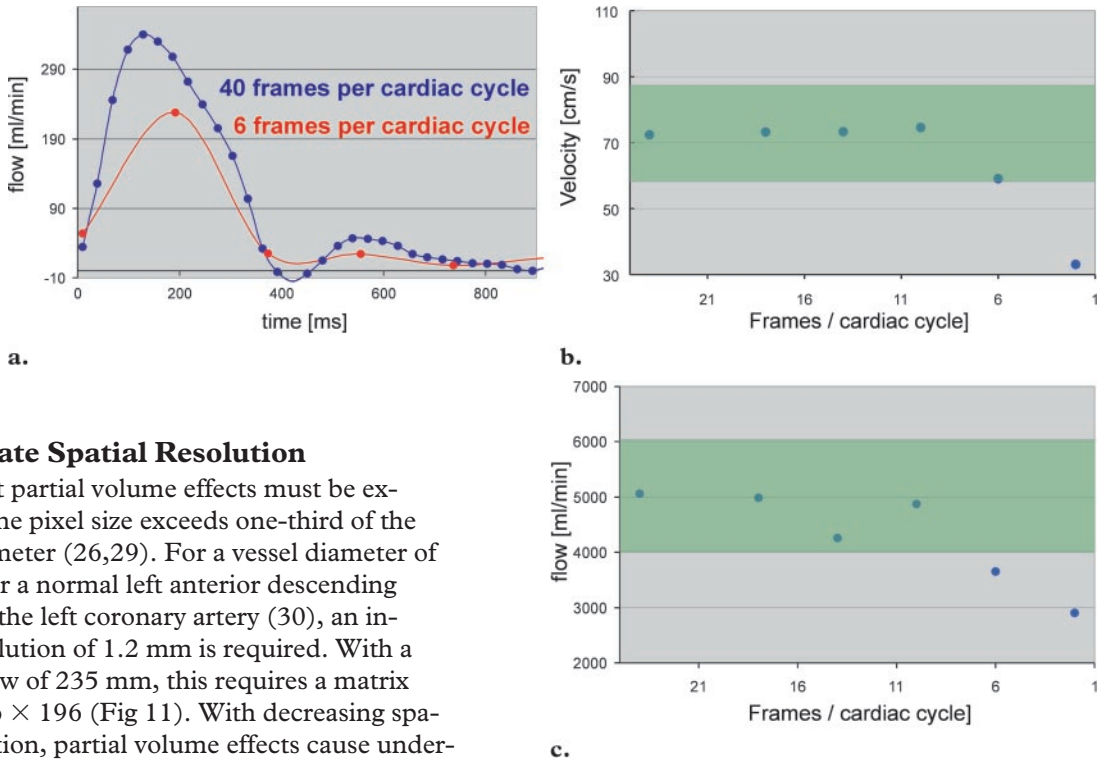

Inadequate Spatial Resolution

Significant partial volume effects must be expected if the pixel size exceeds one-third of the vessel diameter (26,29). For a vessel diameter of 3.6 mm for a normal left anterior descending branch of the left coronary artery (30), an in-plane resolution of 1.2 mm is required. With a field of view of 235 mm, this requires a matrix size of 196 × 196 (Fig 11). With decreasing spatial resolution, partial volume effects cause underestimation of the flow and peak velocity. Flow measurements with an inadequate spatial resolution may still be used for qualitative assessment of the flow dynamics in a vessel (eg, for approximation of the coronary flow reserve) (31–33).

When flow or peak velocity is measured in the great vessels of the mediastinum, this error usually does not occur.

Accelerated Flow and Spatial Misregistration

Phase-contrast measurements are optimized for linear flow. Accelerated flow (eg, turbulence or stenotic jets) causes the precision of the flow measurement to decline (12), although this error might be corrected with a short echo time (34).

Unless the patient moves in an uncontrolled manner, errors resulting from patient movement or other types of spatial misregistration are negligible due to the use of electrocardiographic gating and suspended respiration.

A more severe problem might result from pulsation artifacts of the ascending or descending aorta in the phase-encoding direction (Fig 12). They are most obvious in the velocity images and can be explained by motion of the arteries in the very short interval between the two interleaved data acquisitions used for flow encoding. Sometimes it helps to repeat the measurement after changing the orientations of the phase and frequency encoding.

Figure 11. Inadequate spatial resolution. In an experiment with constant laminar flow of −2,200 mL/min, the spatial resolution decreased from 293 voxels in the vessel diameter at an 18-cm field of view to 66 voxels at a 44-cm field of view. Graphs of the peak velocity **(a)** and flow **(b)** show that flow rates are more sensitive to inadequate spatial resolution. Green area indicates a deviation of ±10% from the peak velocity or flow at the highest spatial resolution used.

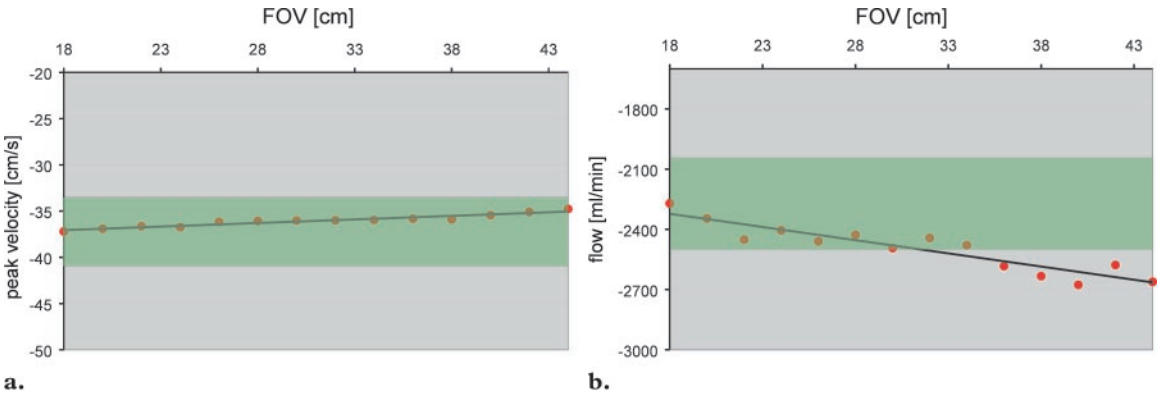

a. b.

Figure 12. Pulsation artifacts in flow measurements. **(a)** Magnitude image (left) shows the phase-encoding direction. Velocity image (right) shows gross pulsation artifacts from the ascending aorta that affect the signal of the superior vena cava (SVC) (red area in both images). **(b)** Magnitude image (left) shows that the phase- and frequency-encoding directions have been switched. Velocity image (right) shows that the artifacts are smaller and do not affect the signal of the SVC (blue area in both images). **(c)** Graph shows flow curves for both measurements. The red curve shows strong deviation from the normal flow curve of the SVC (blue curve) owing to pulsation artifacts, resulting in a false estimate of blood flow.

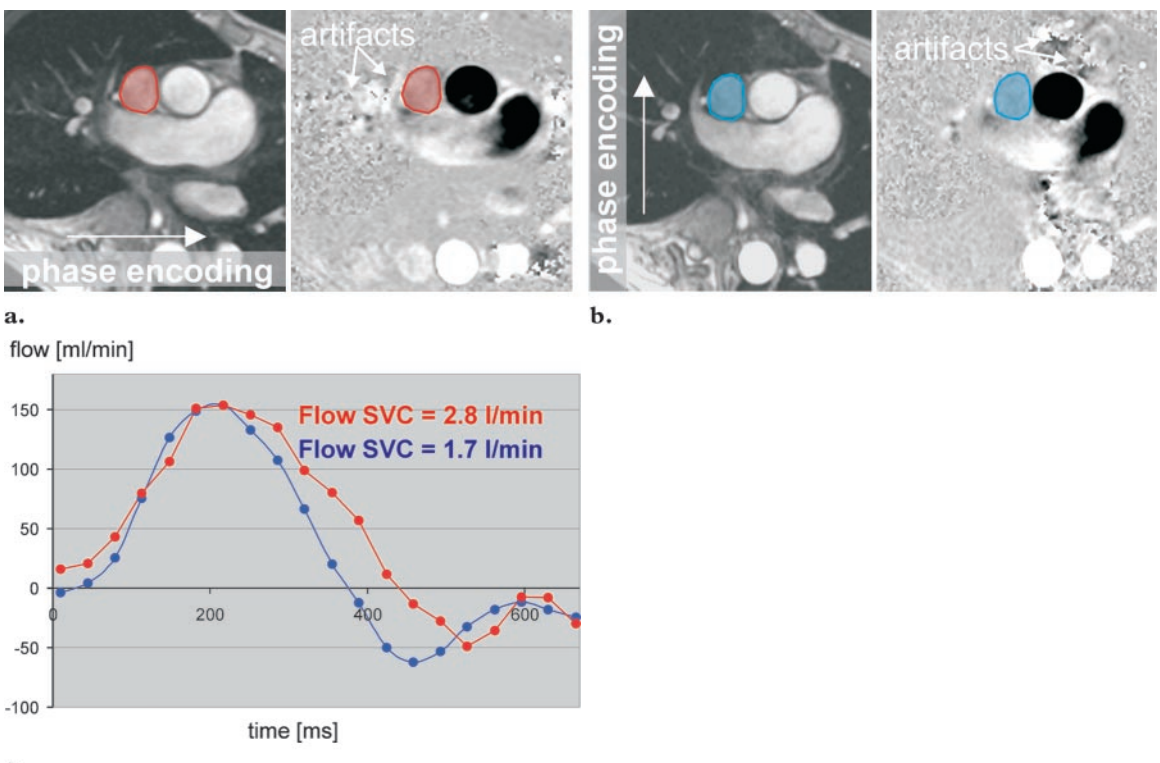

a. b.

c.

Phase Offset Errors

Small phase offset errors are present in almost any clinical MR imaging system. Phase offset error is a systematic phase error of stationary as well as moving spins. The extent of phase offset error is largely dependent on local magnetic field inhomogeneities or gradient imbalance. This error is insidious, since it usually is not constant over the whole field of view. It may be detected if the software for analysis supports a profile representation of the velocity images. In some cases, it may be compensated for by thoroughly applied background subtraction (12). (For details, see the discussion of background compensation later in this article.)

Guidelines for Measurement and Data Analysis

Guidelines for Series Prescription

As pointed out earlier, flow measurements are most precise if the imaging plane is perpendicular to the vessel of interest and flow encoding is set to through-plane flow. Some imaging units have the option of reconstructing the components of flow in each of the three imaging axes separately instead of producing one summarized data set comprising the net through-plane flow. This option is rarely used in routine clinical applications, since most of the software available for flow analysis does not support analysis of the resulting three data sets. However, with special software, this option can be used (eg, to visualize flow trajectories in a vessel).

Use a section thickness of 7 mm to minimize partial volume effects but maintain a good signal-to-noise ratio in the magnitude image. For small vessels like the coronary arteries or renal arteries, the section thickness should be reduced to adapt the partial volume effects to the smaller vessel diameter. How far the section thickness can be reduced before noise deteriorates the measurements depends on the MR imaging unit. For our unit (CV/i system; GE Medical Systems), we use a 5-mm section thickness for the renal arteries, hepatic arteries, and coronary arteries. The choice of the field of view and matrix is closely related to the anatomy.

For precise flow measurements, the sequence has to be repeated at least once. For the first measurement, use a high V_{enc} (see the specific protocols later in this article). A quick analysis of the data will give one an idea of the peak velocities encountered in the vessel. Adding 10% (or a standard 30 cm/sec) to the highest velocity detected will take into account the physiologic variation of the peak velocity during measurement. This procedure is mandatory for estimation of peak velocities.

Check the resulting velocity images for aliasing, phase repetition artifacts, and signal intensity within the vessel of interest. Check the magnitude images for appropriate vessel shape (arteries should be round) and phase wrap artifacts. Phase wrap does not significantly affect the precision of the measurements as long as ghosting is not superimposed on the vessel of interest.

The image or images used to prescribe a phase-contrast measurement should be documented so that errors in imaging plane prescription can be recognized retrospectively. All clinical MR imaging units offer the option of cross-referencing one image into another: The result is a line drawn into the reference image that indicates the calculated projection of the imaging plane of another image into the reference image. This cross-reference can be used at any time during or after the examination. An image should be cross-referenced only to the localizing image used for its prescription. Otherwise, the cross-reference might be misleading in terms of the imaging plane orientation or even the anatomic structure examined. This can be of importance, especially in the

case of double oblique imaging planes in areas of complex anatomy, like the pulmonary veins proximal to the left atrium.

Guidelines for Data Analysis

Special software is required to extract the information from the velocity images. This software can usually be obtained from the vendors of the MR imaging unit; it can also be obtained from independent companies like Medis (Leiden, The Netherlands). Some research sites offer suitable software packages at little or no cost (35).

These programs usually support the drawing of contours (ROIs) into the vessel of interest and automatically copy the contours from magnitude to velocity images and vice versa. The automatic contour detection works reasonably well with large vessels like the aorta or pulmonary vessels. Be sure to use an analysis program that allows ROI shape and position to be adapted for each phase of the cardiac cycle.

Define contours in the magnitude images and always cross-check them in the velocity images. Partial volume effects or large movements of the vessel may result in inadequate contour definition in the magnitude images. This problem may be easily corrected by looking at the velocity images. Experiments have shown that the velocity images can be more reliable for estimation of vessel boundaries than the magnitude images (9,36). This was demonstrated for high systolic flow in the aorta. In the diastolic frames, magnitude images seem to be more suitable for definition of vessel boundaries.

For estimation of the peak velocity, a small ROI within the vessel is sufficient. Indeed, it may give better results than a ROI encompassing the entire vessel, since arbitrary phase values in the tissue adjacent to the vessel are avoided (37). It might help to use profile plots to ensure that the ROI encompasses the area of maximum velocity in the vessel.

As with all quantitative data, the results of flow measurement should be thoroughly correlated with the clinical information, since ROI placement is a user-dependent step in the analysis and may result in erroneous values (38).

Background Compensation

Software packages for phase-contrast flow analysis usually have the option of background subtraction. This option can be used principally to compensate for increased background noise, obvious phase offset errors, or systematic movement of structures like the valve annulus. In technical terms, an additional area is defined by the user or by the program itself to represent noise or the phase offset. The mean phase information of this area is subtracted from the ROI of the vessel. The background area should be as large as possible. It should be in close vicinity to the ROI so that it can compensate for local phase errors and must not include blood vessels or air. These criteria are easily met in the abdomen or extremities but are difficult to maintain within the mediastinum or the heart itself.

Although it is a powerful tool, background compensation should be used with great caution, since it may well introduce more phase errors than it compensates for. There is no simple way to determine the accuracy of background compensation used in an individual case. We avoid using background compensation and limit its use to the rare cases in which large phase offset errors are suspected or noise is obviously high in the velocity images. When it is used, we add a rim of 2–4 voxels around the drawn contour of the vessel for background compensation, depending on the anatomic situation around the vessel of interest. The idea is to bring the contour for background compensation as close as possible to the vessel of interest. It is difficult to use a rim of more than 4–6 voxels because of the proximity of adjacent vascular structures or air space within the mediastinum (Fig 13). If the ROI is smaller than the vessel, a long and thin contour near the vessel wall is used. Profile charts of selected areas can be helpful by providing an impression of the phase shifts or background noise in the velocity images (Fig 13).

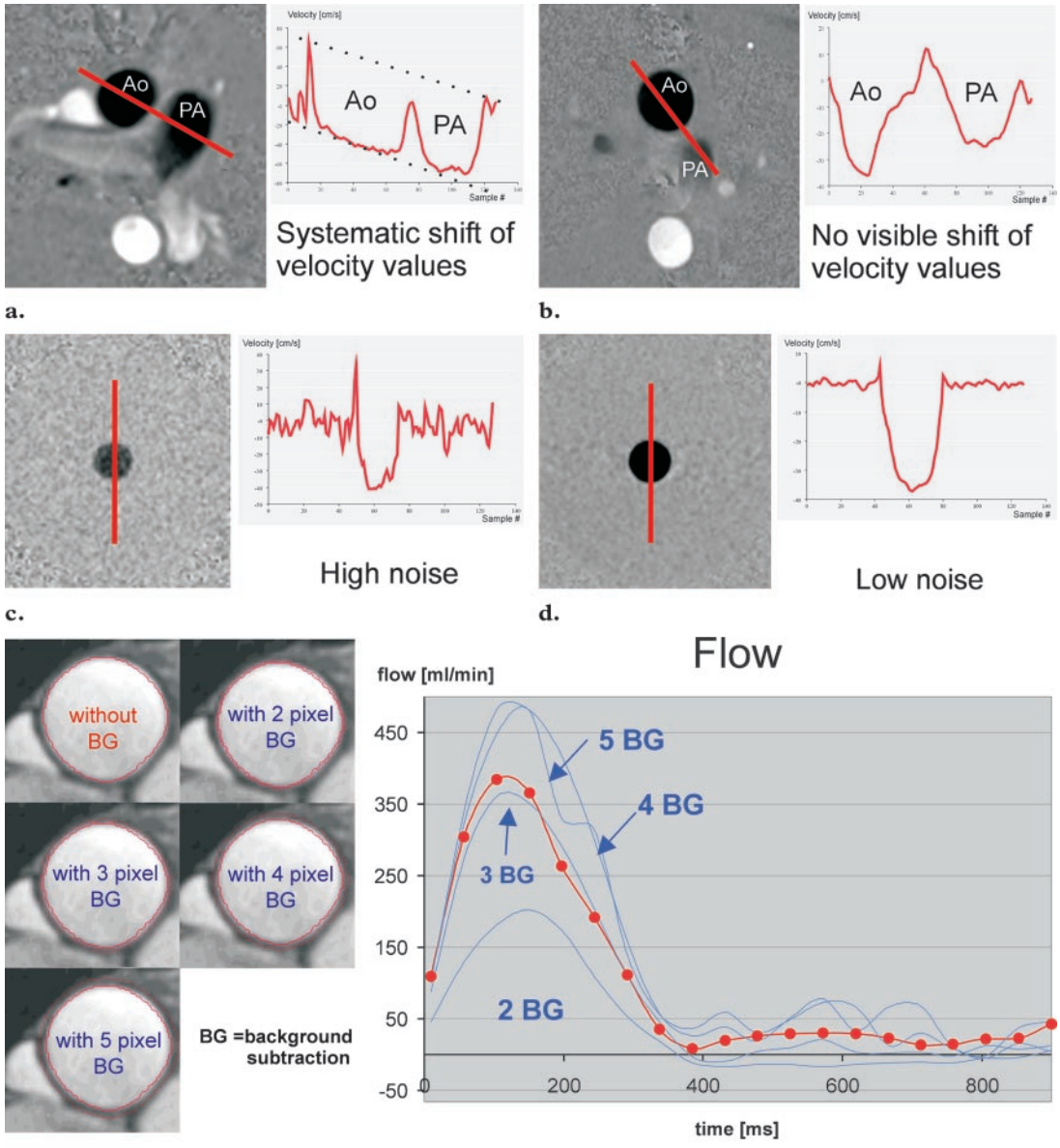

Figure 13. Use of background subtraction in the presence of obvious phase offset errors or obvious noise in the velocity images. **(a)** Velocity image (left) and velocity profile (right) of the aorta (*Ao*) and pulmonary artery (*PA*) show gross phase offset error. In **a–d**, the red line in the velocity image corresponds to the velocity profile. **(b)** Velocity image (left) and velocity profile (right) of the aorta (*Ao*) and pulmonary artery (*PA*) in another patient show normal results. **(c, d)** Velocity image (left) and velocity profile (right) show high noise **(c)** versus low noise **(d)**. **(e)** Graph (right) shows flow curves for the patient shown in **a**. The flow curves were created with increasing background subtraction, as indicated in the corresponding images (left). Even minor changes in the degree of background subtraction can result in large deviations in estimated flow; there is no way to judge what extent of background correction is optimal on the basis of flow measurement images alone. Therefore, background compensation should be used sparingly.

Sequence and Parameters Used for Phase-Contrast Flow Measurement

Sequence	FastCine PC*
k-space segmentation (views per segment)	4–12†
View-sharing interpolation (reconstructed frames per cardiac cycle)	30
Velocity encoding (cm/sec)	30–550
Field of view (mm)	260–340‡
Matrix	256 × 160
Section thickness (mm)	7
Repetition time (msec)	7§
Echo time (msec)	3.7§
Signals acquired	1
Flip angle (degrees)	40
Imaging time (sec)	<24‖

*GE Medical Systems. Retrospective electrocardiographic gating and view-sharing interpolation are also used.
†Depends on the heart rate and the ability to breath hold.
‡Depends on the size of the patient, the imaging plane selected, and the surface coil used.
§Minimum values are used for all measurements.
‖Depends largely on the pulse rate and the k-space segmentation.

Specific Protocols

These protocols represent our experience with flow measurement using a 1.5-T MR imaging unit (CV/i and Signa Horizon; GE Medical Systems). Modifications for routine daily use might be necessary, depending on the individual imaging unit and the available software. The sequence parameters used in the following examples are listed in the Table.

Use of minimum values for repetition time and echo time improves the temporal resolution and image quality. Use of minimum values for echo time makes the measurements less sensitive to motion artifacts and turbulent flow but also reduces the signal-to-noise ratio of the measurement. Therefore, it might be necessary to increase the echo time to control excessive noise in the images, depending on the MR imaging system used.

With the parameters given, the time needed to complete a measurement is controlled by variation of the k-space segmentation (the views per segment). An imaging time of 20 seconds or less is desirable for both patient comfort and reproducibility of the measurements.

As stated earlier, we repeat flow measurements with an adapted V_{enc} if peak velocities have to be estimated.

SVC and Inferior Vena Cava

The encoding velocity for the first measurement or for flow measurement is 110 cm/sec. The usual velocity for peak velocity measurement is 50–80 cm/sec.

For the SVC, select an imaging plane below the influx of the azygos vein. The azygos vein must be visible in the magnitude image. For the inferior vena cava (IVC), select an imaging plane above the hepatic vein influx. If in doubt, choose a plane in the lower end of the right atrium, which usually covers the ventral wall of the IVC.

The SVC is usually triangular when imaged at or below the pulmonary bifurcation (Fig 14). The shape of the IVC is very variable, from slitlike to circular.

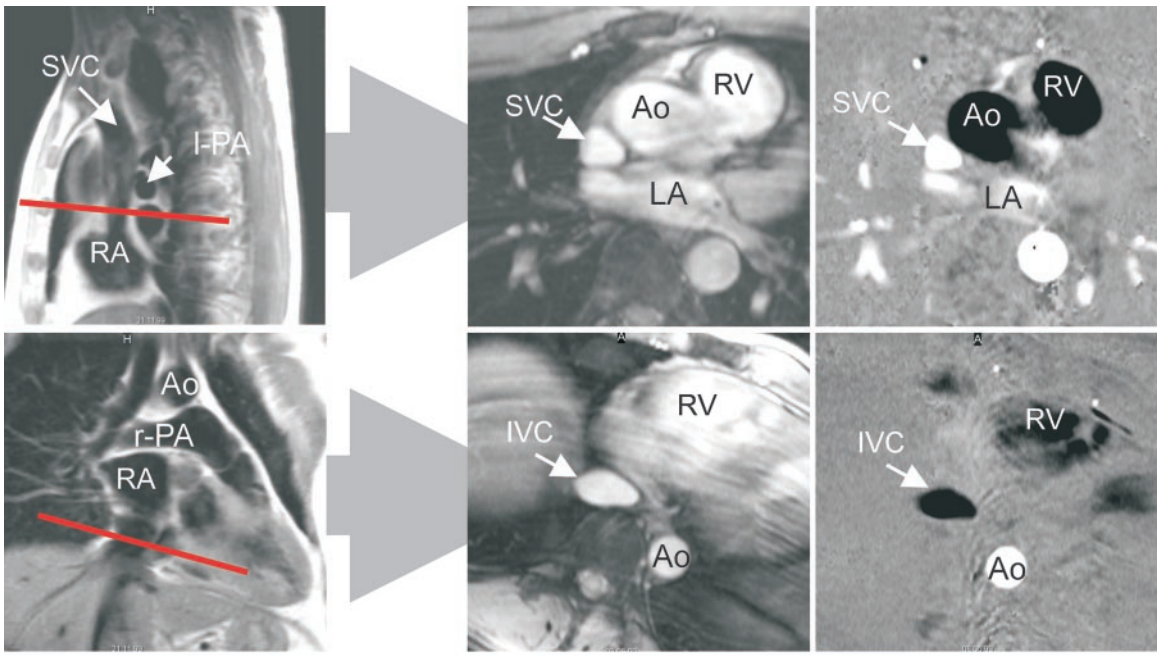

a.

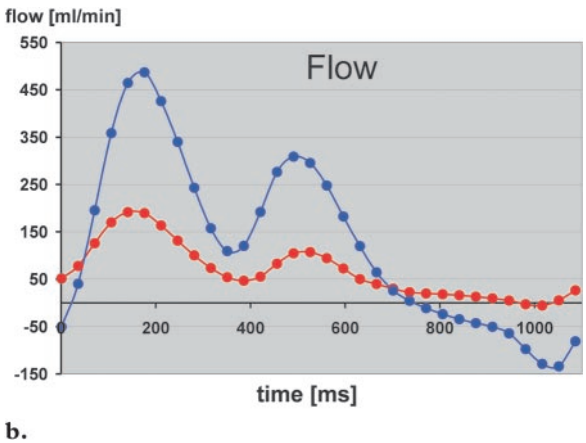

b.

Figure 14. SVC and IVC. **(a)** Localizing (left), magnitude (middle), and velocity (right) images show a normal SVC (top) and IVC (bottom). Red line in the localizing image indicates the imaging plane of the flow images. *Ao* = aorta, *LA* = left atrium, *l-PA* = left pulmonary artery, *RA* = right atrium, *r-PA* = right pulmonary artery, *RV* = right ventricle. **(b)** Graph shows estimates of flow in the SVC (red line) and IVC (blue line).

Ascending Aorta

The encoding velocity for the first measurement or for flow measurement is 200 cm/sec. The usual velocity for peak velocity measurement is 100–160 cm/sec.

Select the imaging plane on an oblique sagittal localizing image that shows the ascending aorta (Fig 15). We prefer an imaging plane at the level of the pulmonary bifurcation, since it is easy to reproduce. This imaging plane also has sufficient distance from the aortic valve so that the effect of mild valvular disease does not disturb the flow measurements. If the flow measurement is to be performed in suspended respiration, the localizing image should also be acquired in suspended respiration to avoid gross anatomic deviation of the imaging plane.

The diastolic flow into the coronary arteries is approximately 0.5% of the cardiac output (39). As the error of the measurement itself is far beyond this value, coronary distribution need not be compensated for when estimating the cardiac output from the flow in the ascending aorta.

Repetition artifacts from the descending aorta are quite often encountered in the systolic frames of the cardiac cycle. If the artifacts project into the ascending aorta, we prefer to repeat the measurement with the frequency-encoding axis in the anterior-posterior orientation. The field of view must be enlarged in this case to avoid significant phase wrap artifacts.

Main Pulmonary Artery

The encoding velocity for the first measurement or for flow measurement is 180 cm/sec. The usual velocity for peak velocity measurement is 60–120 cm/sec.

Use an oblique localizer on an axial or coronal image to visualize the natural bowing of the pulmonary artery (Fig 16). On the resulting image, select an imaging plane above the pulmonary valve but below the pulmonary bifurcation. The

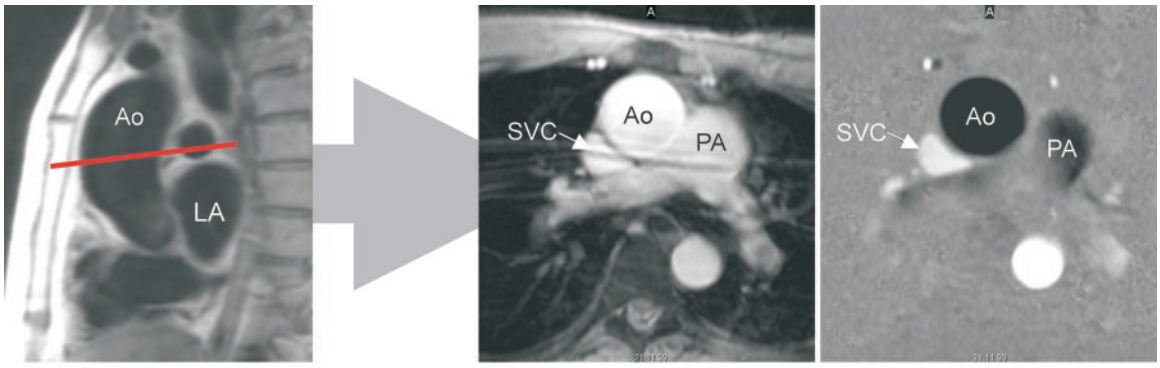

a.

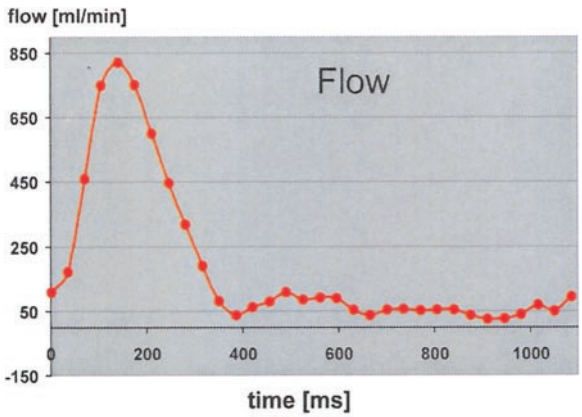

b.

Figure 15. Ascending aorta. **(a)** Localizing (left), magnitude (middle), and velocity (right) images show a normal ascending aorta (*Ao*). The imaging plane is prescribed in an oblique sagittal localizing image (red line). *LA* = left atrium, *PA* = pulmonary artery. **(b)** Graph shows estimates of flow in the ascending aorta.

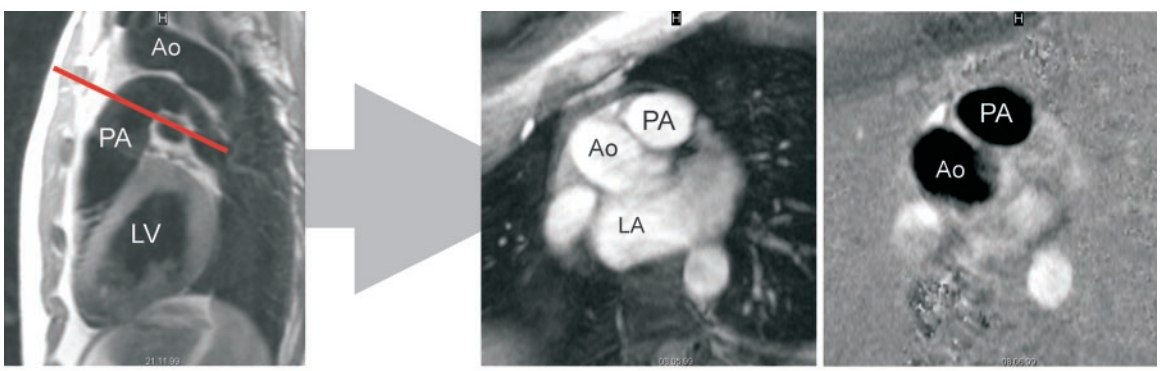

a.

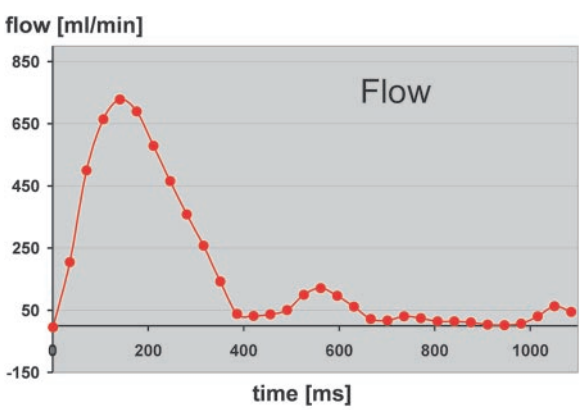

b.

Figure 16. Main pulmonary artery. **(a)** Localizing (left), magnitude (middle), and velocity (right) images show a normal pulmonary artery (*PA*). Red line in the localizing image indicates the imaging plane of the flow images. *Ao* = aorta, *LA* = left atrium, *LV* = left ventricle. **(b)** Graph shows estimates of flow in the pulmonary artery.

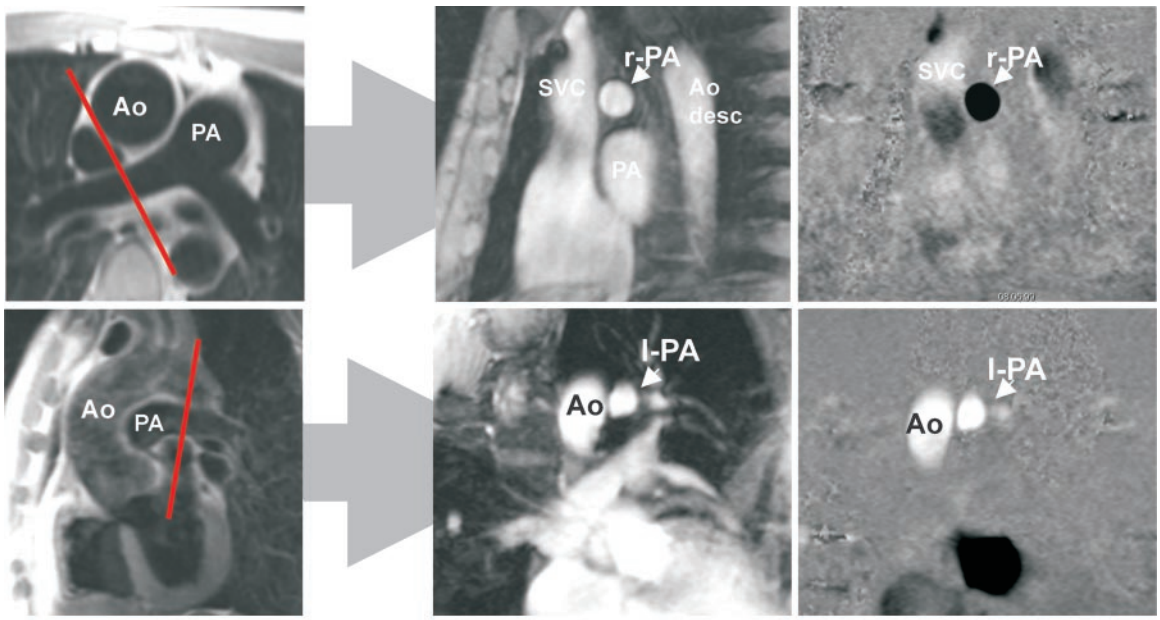

a.

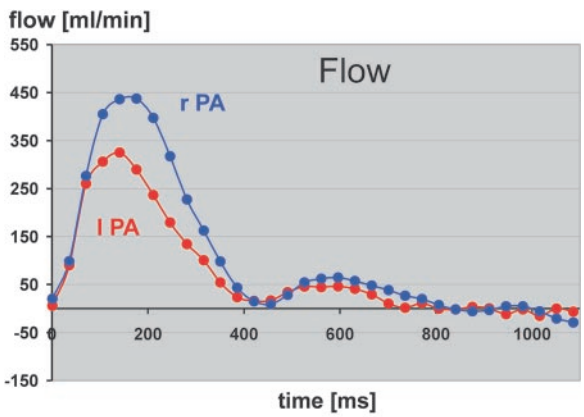

b.

Figure 17. Right and left pulmonary arteries. **(a)** Localizing (left), magnitude (middle), and velocity (right) images show the right pulmonary artery (*r-PA*) (top) and left pulmonary artery (*l-PA*) (bottom). In the localizing image for the right pulmonary artery (top left), the imaging plane (red line) is selected to avoid the trachea and aorta (*Ao*). In the localizing image for the left pulmonary artery (bottom left), the imaging plane (red line) is selected to avoid the upper lobe artery. *desc* = descending, *PA* = main pulmonary artery. **(b)** Graph shows estimates of flow in the right (*r PA*) and left (*l PA*) pulmonary arteries.

choice of the localizer for the pulmonary trunk is crucial. It sometimes helps to choose a plane in the right ventricular outflow tract to visualize the pulmonary valve and pulmonary bifurcation.

Reliable measurement in the pulmonary trunk may be difficult. The distance between the pulmonary valve and the pulmonary bifurcation is usually less than 2 cm. It might help to measure the flow in the right and left pulmonary arteries and add both values for the cardiac output of the right ventricle.

Right and Left Pulmonary Arteries

The encoding velocity for the first measurement or for flow measurement is 200 cm/sec. The usual velocity for peak velocity measurement is 60–120 cm/sec.

For the right pulmonary artery, use an oblique localizer on an axial or coronal image (Fig 17). The best plane is between the trachea and the ascending aorta. For the left pulmonary artery, use an oblique localizer on an axial image. With the final localizer, stay close to the pulmonary trunk to avoid the left upper lobe artery.

In a healthy adult, 55% of pulmonary flow goes through the right pulmonary artery and 45% goes through the left pulmonary artery (40).

Small Intracardiac Structures

For small structures (shunts, grafts, bypasses), spatial resolution and temporal resolution are the most important sources of errors (41). The coronary arteries and the coronary sinus pose an additional problem because of their complex movement (42). Qualitative flow curve estimation may be performed for even very small structures. The smaller the structure of interest, the more important thorough plane selection and documentation become. Especially if the study results have to be

reevaluated afterward, it might be impossible to interpret them if no clear documentation of the imaging plane was done.

As is true for all flow measurements performed in a breath hold, small intracardiac structures should be evaluated in suspended expiration. With prospective cardiac gating, acquisition of four to seven frames per cardiac cycle is typically feasible in one breath hold of 20 seconds when a pixel resolution of 0.82–0.94 mm is used (33). Sequences that use retrospective cardiac gating and view-sharing interpolation can produce more than 30 frames per cardiac cycle in a single breath hold, like the FastCine sequence (GE Medical Systems) used for the protocols given herein. Especially for coronary arteries like the left anterior descending branch, it helps to choose only the anterior coil elements of a phased-array coil for image reconstruction. This allows reduction of the field of view to about 22–24 cm without inducing significant artifacts from phase wrap of the posterior chest wall elements.

Whenever measurements are performed in a breath hold, one should keep in mind that a prolonged breath hold affects hemodynamics and may alter results even for qualitative measurements (43).

Combined Protocols

Cardiac Output.—Determination of cardiac output can be easily performed with phase-contrast measurement. As an internal control of the measurement, we always determine the cardiac output of the left ventricle in the ascending aorta and compare it with the cardiac output of the right ventricle in the pulmonary trunk. Gross differences between these two measurements indicate an error in prescription (most often) or an unknown intra- or extracardiac shunt (quite seldom).

Quantification of known intracardiac shunts with the volume load of the pulmonary circulation can be performed by comparison of the cardiac outputs of the left and right ventricles as determined by flow measurements in the aorta and pulmonary artery (44).

Aortic Coarctation.—Evaluation of aortic coarctation is a strong indication for MR imaging and for MR flow measurement. As proposed by Steffens et al (6) and others (45), the collateral flow in aortic coarctation can be assessed by measuring the blood flow within 2 cm of the coarctation and above the diaphragm. In the healthy patient, a decrease in flow can be expected because of antegrade perfusion of the intercostal arteries from the aorta. In significant coarctation, the flow increases from within the coarctation toward the diaphragm due to retrograde perfusion of the intercostal arteries, which serve as a source of collateral flow.

Although Steffens et al (6) and others (45) suggested an imaging plane above the coarctation as a primary baseline for assessment of collateral flow, we prefer using a plane within 2 cm below the coarctation, since this plane is much easier to find. This is especially true for stenoses with little or no distance to the left subclavian artery.

An additional measurement within the coarctation and determination of the peak velocity can help estimate the pressure gradient Δp within the stenosis according to the modified Bernoulli theorem:

$$\Delta p = 4 \cdot (V_{max})^2. \quad (4)$$

V_{max} must have the dimension of meters per second to result in the correct pressure gradient, which has the dimension of millimeters of mercury (mm Hg).

As mentioned earlier, we use two flow measurements to evaluate the pressure gradient in aortic coarctation. The first measurement is performed with high V_{enc} values, starting with 400 cm/sec (or a pressure gradient of 64 mm Hg). A pressure gradient of more than 20 mm Hg as measured during cardiac catheterization is considered an indication for intervention (46). Therefore, a pressure drop of more than 20 mm Hg (or $V_{max} > 220$ cm/sec) in the phase-contrast measurement is a significant finding.

Conclusions

When the recommendations and protocols presented herein are kept in mind, phase-contrast flow measurement is easy to perform and yields reliable results. In contrast to the results of other techniques, the results of phase-contrast flow measurement can be reevaluated with the same reliability at any time. This is an important prerequisite for standardized and long-term quality assurance of quantitative measurements.

The overall error for MR flow measurement in the great vessels—including prescription and data analysis—can be less than 10%.

Progress in sequence design promises higher temporal and spatial resolution. We might see real-time flow measurement as a commercially

available software option for MR imaging units within the next 2 years, which will further broaden indications for flow measurement in cardiac MR imaging. Real-time phase-contrast flow measurement techniques have been reported as research work since the early 1990s (47–49), with quite acceptable temporal and spatial resolution in the more recent reports (50,51).

The principle of quantitative phase-contrast measurement is not limited to blood flow measurement but can be applied to any kind of motion. There have been promising studies on use of phase-contrast imaging for analysis of myocardial wall motion (52,53).

There is still a lack of studies with large patient numbers that compare MR flow measurement with other invasive or noninvasive techniques. Therefore, the usefulness of quantitative MR flow measurement is still not adequately appreciated by radiologists as well as our clinical partners, who have to trust our results if we want them to include this technique in their daily work.

References

1. Maier SE, Meier D, Boesiger P, Moser UT, Vieli A. Human abdominal aorta: comparative measurements of blood flow with MR imaging and multigated Doppler US. Radiology 1989; 171: 487–492.
2. Moran PR. A flow zeugmatographic interlace for NMR imaging in humans. Magn Reson Imaging 1982; 1:197–203.
3. O'Donnell M. NMR blood flow using multiecho, phase contrast sequences. Med Phys 1985; 12:59–64.
4. Singer JR. Blood flow rates by NMR measurements. Science 1959; 130:1652–1653.
5. Sakuma H, Kawada N, Takeda K, Higgins CB. MR measurement of coronary blood flow. J Magn Reson Imaging 1999; 10:728–733.
6. Steffens JC, Bourne MW, Sakuma H, O'Sullivan M, Higgins CB. Quantification of collateral blood flow in coarctation of the aorta by velocity encoded cine magnetic resonance imaging. Circulation 1994; 90:937–943.
7. Kayser HW, Stoel BC, van der Wall EE, van der Geest RJ, de Roos A. MR velocity mapping of tricuspid flow: correction for through-plane motion. J Magn Reson Imaging 1997; 7:669–673.
8. Hundley WG, Li HF, Lange RA, et al. Magnetic resonance imaging assessment of the severity of mitral regurgitation: comparison with invasive techniques. Circulation 1995; 92:1151–1158.
9. Moran PR, Moran RA, Karstaedt N. Verification and evaluation of internal flow and motion. Radiology 1985; 154:433–441.
10. Spritzer CE, Pelc NJ, Lee JN, Evans AJ, Sostman HD, Riederer SJ. Rapid MR imaging of blood flow with a phase-sensitive, limited-flip-angle, gradient recalled pulse sequence: preliminary experience. Radiology 1990; 176:255–262.
11. O'Donnell M. NMR blood flow imaging using multiecho, phase contrast sequences. Med Phys 1985; 12:59–64.
12. Bakker CJ, Hoogeveen RM, Viergever MA. Construction of a protocol for measuring blood flow by two-dimensional phase-contrast MRA. J Magn Reson Imaging 1999; 9:119–127.
13. Evans AJ, Iwai F, Grist TA, et al. Magnetic resonance imaging of blood flow with a phase subtraction technique. Invest Radiol 1993; 28:109–115.
14. Kondo C, Caputo GR, Semelka R, Foster E, Shimakawa A, Higgins CB. Right and left ventricular stroke volume measurements with velocity encoded cine MR imaging: in vitro and in vivo validation. AJR Am J Roentgenol 1991; 157:9–16.
15. Hoeper MM, Tongers J, Leppert A, Baus S, Maier R, Lotz J. Evaluation of right ventricular performance with a right ventricular ejection fraction thermodilution catheter and magnetic resonance imaging in patients with pulmonary hypertension. Chest 2001; 120:502–507.
16. Heerdt PM, Blessios GA, Beach ML, Hogue CW. Flow dependency of error in thermodilution measurement of cardiac output during acute tricuspid regurgitation. J Cardiothorac Vasc Anesth 2001; 15:183–187.
17. Heerdt PM, Pond CG, Blessios GA, Rosenbloom M. Comparison of cardiac output measured by intrapulmonary artery Doppler, thermodilution, and electromagnetometry. Ann Thorac Surg 1992; 54:959–966.
18. Globits S, Pacher R, Frank H, et al. Comparative assessment of right ventricular volumes and ejection fraction by thermodilution and magnetic resonance imaging in dilated cardiomyopathy. Cardiology 1995; 86:67–72.
19. Gamroth AH, Schad LR, Wacker CM, et al. Measurement of the blood flow velocity in the pulmonary arteries using the magnetic resonance technique. Radiologe 1992; 32:182–184. [German]
20. Lee VS, Spritzer CE, Caroll BA, et al. Flow quantification using fast cine phase-contrast MR imaging, conventional cine phase-contrast MR imaging, and Doppler sonography: in vitro and in vivo validation. AJR Am J Roentgenol 1997; 12:1952–1953.
21. Hoskins PR. Accuracy of maximum velocity estimates made using Doppler ultrasound systems. Br J Radiol 1996; 69:172–177.
22. Sadek AG, Mohamed FB, Outwater EK, El-Essawy SS, Mitchell DG. Respiratory and postprandial changes in portal flow rate: assessment by phase contrast MR imaging. J Magn Reson Imaging 1996; 6:90–93.
23. Buonocore MH. Blood flow measurement using variable velocity encoding in the RR interval. Magn Reson Med 1993; 28:790–795.
24. Andersen AH, Kirsch JE. Analysis of noise in phase contrast MR imaging. Med Phys 1996; 23: 857–869.
25. Yang GZ, Burger P, Kilner PJ, Karwatowski SP, Firmin DN. Dynamic range extension of cine velocity measurements using motion-registered spatiotemporal phase unwrapping. J Magn Reson Imaging 1996; 6:495–502.
26. Tang C, Blatter DD, Parker DL. Accuracy of phase contrast flow measurements in the presence of partial-volume effects. J Magn Reson Imaging 1993; 3:377–385.
27. Polzin JA, Frayne R, Grist TM, Mistretta A. Frequency response of multi-phase segmented k-space phase-contrast. Magn Reson Med 1996; 35:755–762.

28. Foo TK, Bernstein MA, Aisen AM, Hernandez RJ, Collick BD, Bernstein T. Improved ejection fraction and flow velocity estimates with use of view sharing and uniform repetition time excitation with fast cardiac techniques. Radiology 1995; 195:471–478.
29. Hofman MBM, Visser FC, van Rossum AC, Vink GQM, Sprenger M, Westerhof N. In vivo validation of magnetic resonance blood volume flow measurements with limited spatial resolution in small vessels. Magn Reson Med 1995; 33:778–784.
30. Leung WH, Stadius ML, Alderman EL. Determinants of normal coronary artery dimensions in humans. Circulation 1991; 84:2294–2306.
31. Hundley WG, Hillis LD, Hamilton CA, et al. Assessment of coronary arterial restenosis with phase-contrast magnetic resonance imaging measurements of coronary flow reserve. Circulation 2000; 101:2375–2381.
32. Schwitter J, DeMarco T, Kneifel S, et al. Magnetic resonance-based assessment of global coronary flow and flow reserve and its relation to left ventricular functional parameters: a comparison with positron emission tomography. Circulation 2000; 101:2696–2702.
33. Hundley WG, Hamilton AC, Clarke GD, et al. Visualization and functional assessment of proximal and middle left anterior descending coronary stenoses in humans with magnetic resonance imaging. Circulation 1999; 99:3248–3254.
34. Mohiaddin RH, Gatehouse PD, Henien M, Firmin DN. Cine MR Fourier velocimetry of blood flow through cardiac valves: comparison with Doppler echocardiography. J Magn Reson Imaging 1997; 7:657–663.
35. Graves MJ, Brewin MP, Priest AN, Coulden RAR. Automated analysis of cine phase contrast velocity images using score guided erosion (abstr). In: Proceedings of the Ninth Meeting of the International Society for Magnetic Resonance in Medicine. Berkeley, Calif: International Society for Magnetic Resonance in Medicine, 2001; 835.
36. Kozerke S, Botnar R, Oyre S, Scheidegger MB, Pedersen EM, Boesiger P. Automatic vessel segmentation using active contours in cine phase contrast flow measurements. J Magn Reson Imaging 1999; 10:41–51.
37. Hamilton CA, Moran PR, Santago P 2nd, Rajala SA. Effects of intravoxel velocity distributions on the accuracy of the phase mapping method in phase-contrast MR angiography. J Magn Reson Imaging 1994; 4:752–755.
38. Burkart DJ, Felmlee JP, Johnson CD, et al. Cine phase-contrast MR flow measurements: improved precision using an automated method of vessel detection. J Comput Assist Tomogr 1994; 18: 469–475.
39. Mymin D, Sharma GP. Total and effective coronary blood flow in coronary and noncoronary heart disease. J Clin Invest 1974; 53:363–373.
40. Henk CB, Schlechta B, Grampp S, Gomischek G, Klepetko W, Mostbeck GH. Pulmonary and aortic blood flow measurements in normal subjects and patients after single lung transplantation at 0.5 T using velocity encoded cine MRI. Chest 1998; 114:771–779.
41. Sakuma H, Globits S, O'Sullivan M, et al. Breathhold MR measurements of blood flow velocity in internal mammary arteries and coronary artery bypass grafts. J Magn Reson Imaging 1996; 6: 219–222.
42. Clarke GD, Hundley WG, McColl RW, et al. Velocity-encoded, phase-difference cine MRI measurements of coronary artery flow: dependence of flow accuracy on the number of cine frames. J Magn Reson Imaging 1996; 6:733–742.
43. Sakuma H, Kawada N, Kubo H, et al. Effect of breath holding on blood flow measurement using fast velocity encoded cine MRI. Magn Reson Med 2001; 45:346–348.
44. Kalden P, Kreitner KF, Voiglander T, et al. Flow quantification of intracardiac shunt volumes using MR phase contrast technique in the breath holding phase. Rofo Fortschr Geb Rontgenstr Neuen Bildgeb Verfahr 1998; 169:378–382. [German]
45. Chernoff DM, Derugin N, Rajasinghe HA, Hanley FL, Higgins CB, Gooding CA. Measurement of collateral blood flow in a porcine model of aortic coarctation by velocity-encoded cine MRI. J Magn Reson Imaging 1997; 7:557–563.
46. Campbell M. Natural history of coarctation of the aorta. Br Heart J 1970; 32:633–640.
47. Wetzel SG, Lee VS, Tan AG, et al. Real-time interactive duplex MR measurements: application in neurovascular imaging. AJR Am J Roentgenol 2001; 177:703–707.
48. Eichenberger AC, Schwitter J, McKinnon GC, Debatin JF, von Schulthess GK. Phase-contrast echo-planar MR imaging: real-time quantification of flow and velocity patterns in the thoracic vessels induced by Valsalva's maneuver. J Magn Reson Imaging 1995; 5:648–655.
49. Moller HE, Klocke HK, Bongartz GM, Peters PE. MR flow quantification using RACE: clinical application to the carotid arteries. J Magn Reson Imaging 1996; 6:503–512.
50. Nayak KS, Pauly JM, Kerr AB, Hu BS, Nishimura DG. Real-time color flow MRI. Magn Reson Med 2000; 43:251–258.
51. Man LC, Pauly JM, Nishimura DG, Macovski A. Nonsubtractive spiral phase contrast velocity imaging. Magn Reson Med 1999; 42:704–713.
52. Kayser HW, van der Geest RJ, van der Wall EE, Duchateau C, de Roos A. Right ventricular function in patients after acute myocardial infarction assessed with phase contrast MR velocity mapping encoded in three directions. J Magn Reson Imaging 2000; 11:471–475.
53. Pelc LR, Sayre J, Yun K, et al. Evaluation of myocardial motion tracking with cine-phase contrast magnetic resonance imaging. Invest Radiol 1994; 29:1038–1042.